La mer 30: 229–238, 1992
Société franco-japonaise d'océanographie, Tokyo

Numerical simulation for a northeastward flowing current from area off the Eastern Hainan Island to Tsugaru/Soya Strait

R. LI*, Q. ZENG*, Z. JI* and D. GUN*

Abstract: The upper-layer monthly-mean circulations in the Pacific Ocean are calculated by using a barotropic ocean model with a fine-horizontal resolution. We focus our attention on a northeastward flowing current which is closely related to the currents in the China Sea and Japan Sea. Simulated results show that, both in winter (January) and summer (July), the northeastward current starts from the region off the eastern Hainan Island, passing through the Taiwan Strait, East China Sea, the Korea Strait and Japan Sea, eventually entering the Pacific Ocean through the Tsugaru Strait in winter, but through the Soya Strait in summer. The distribution of the simulated sea surface elevation reveals that the combined effect of the sea surface slope in the direction of the current and that across the current from southeast to northwest is probably one of the major forces driving the current.

1. Introduction

The China Sea is an ideal monsoon region. A strong north or northeast monsoon blows in winter, while a weak south or southwest monsoon prevails in summer. Therefore, many oceanographers have taken it for granted that under the intense influence of the northerly monsoon in winter, the coastal current off the southeast coast of China flows leeward from northeast to southwest. In the late fifties and early sixties, the results obtained from the Chinese National Comprehensive Oceanographic Survey (1958–1960) denounced the traditional concept above about the coastal current off the southeast coast of China. GUAN *et al.* (1964) pointed out the following:

1. In the offshore region of eastern Zhejiang, besides the East China Sea Coastal Current flowing leeward close to the coast, there exists a current flowing northeastward against the wind in the area a little further away from the coast. They named the current "Taiwan Warm Current" at that time.

2. In the nearshore region of Shantou (east of 116° E), there also exists a current flowing northeastward against the wind. In addition, in the coastal area northeast of the Hainan Island, a windward current is also observed. The northeastward flowing currents observed in two regions mentioned above are considered to be connected with each other and are called the "South China Sea Warm Current."

In the early sixties, GUAN *et al.* (1964) conjectured that there might also exist a northeastward windward current in the deep and near-bottom layers of the western part of the Taiwan Strait, and further suggested that this conjecture should be confirmed by future observations. They also conjectured that besides the leeward cold current in winter there exists a windward current flowing northeastward off the southeast coast of China.

Based on the analysis of the observational data, GUAN (1984, 1986) showed that in winter there exists a windward current from the coastal area east of the Hainan Island, passing through the shore region of eastern Guangdong and the western part of the Taiwan Strait, and reaching the shore region of Fujian and Zhejiang.

GUAN (1986) also pointed out that there exists a water passage through the northeast of the South China Sea, Taiwan Strait, northwest of the East China Sea, the Korea Strait, and thought that this water passage has reference to

* LASG, Institute of Atmospheric Physics, Chinese Academy of Sciences

expounding the source of the Tsushima Warm Current.

FANG *et al.* (1988) indicated that the sea surface elevation difference between the Luzon Strait and the area east of Tsugaru and Soya Strait may induce a current starting from northeast of the South China Sea to Tsugaru/Soya Strait. FANG *et al.* (1989) named it "Taiwan-Tsushima-Tsugaru Warm Current System (TTTWCS)."

During investigating this current, GUAN and FANG could only rely on observations at some limited areas because the current measurements are still very scanty (Fig. 2). It is rather difficult to understand the complete picture of such a long current based only on the insufficient observations. Does this current really exist? If it does, what is the driving mechanism of it? Could it be confirmed by numerical simulations?

In order to answer these questions, numerical calculations have been done by using an ocean model which is the simplest form of the ocean-atmosphere coupling models presented by ZENG (1983). Some theories and methods applicable to numerical weather prediction (NWP) models and general circulation models (GCM) developed by Institute of Atmospheric Physics (IAP) have been incorporated into the model (e.g., ZENG *et al.*, 1987). In addition, techniques saving computational time have also been employed in the model (e.g., ZENG *et al.*, 1985, 1990).

2. Sketch of model

In a colatitude-longitude spherical surface coordinate system (θ, λ, z), the vertically-averaged equations of motion and continuity are adopted:

$$\frac{d\vec{v}}{dt} = -\nabla\phi - f^*\vec{k}^0\times\vec{v} - \kappa_2\vec{v} + \frac{\vec{\tau}}{\rho_0 h} + A_m\left[\Delta\vec{v} + \frac{1-\mathrm{ctg}^2\theta}{a^2}\vec{v} + \frac{2\mathrm{ctg}\,\theta}{a^2\sin\theta}\vec{k}^0\times\frac{\partial\vec{v}}{\partial\lambda}\right] \quad (1)$$

$$\frac{\partial\zeta}{\partial t} + \frac{1}{a\sin\theta}\left(\frac{\partial hv\sin\theta}{\partial\theta} + \frac{\partial hu}{\partial\lambda}\right) = 0, \quad (2)$$

Δ is the Laplacian operator on a sphere; $\vec{v}$ is the depth-averaged velocity vector; $h = h_0 + \zeta$ is the thickness of the water layer, h_0 is the undisturbed water depth, ζ is the sea surface elevation; ϕ $(=g\zeta)$ is the geopotential departure of the free surface; g is the acceleration of gravity: a is the Earth's radius: ρ_0 is the density of the seawater, taking $\rho_0 = 1.024\mathrm{g/cm^3}$; A_m is the lateral eddy viscosity coefficient; κ_2 is the bottom friction coefficient: $f^* = (2\omega\cos\theta + u\mathrm{ctg}\,\theta/a)$ is the apparent Coriolis parameter, ω is the angular speed of the Earth's rotation; $\vec{\tau}$ is the wind strees vector.

In order to design energy conserving time-space finite difference schemes conveniently, we introduce a variable substitution. If we substitute

$$\vec{V} \equiv \phi\vec{v}, \quad \phi \equiv \sqrt{gh_0 + \phi},$$

for $\vec{v} = \vec{\theta}^0 v + \vec{\lambda}^0 u$, Eqs. (1) and (2) can be rewritten as,

$$\frac{\partial\vec{V}}{\partial t} = -L_1(\vec{V}) - L_2(\vec{V}) - \phi\nabla\phi - f^*\vec{k}^0\times\vec{V} - \kappa_2\vec{V} + g\frac{\vec{\tau}}{\rho_0\phi} + A_m\phi\left[\Delta\vec{v} + \frac{1-\mathrm{ctg}^2\theta}{a^2}\vec{v} + \frac{2\mathrm{ctg}\,\theta}{a^2\sin\theta}\vec{k}^0\times\frac{\partial\vec{v}}{\partial\lambda}\right], \quad (3)$$

$$\frac{\partial\phi}{\partial t} = -\frac{1}{a\sin\theta}\left(\frac{\partial\phi V\sin\theta}{\partial\theta} + \frac{\partial\phi U}{\partial\lambda}\right), \quad (4)$$

where

$$L_1(F) \equiv \frac{1}{2a\sin\theta}\left(\frac{\partial Fv\sin\theta}{\partial\theta} + v\sin\theta\frac{\partial F}{\partial\theta}\right),$$

$$L_2(F) \equiv \frac{1}{2a\sin\theta}\left(\frac{\partial Fu}{\partial\lambda} + u\frac{\partial F}{\partial\lambda}\right), \quad (F = V \text{ or } U),$$

The lateral boundary condition is

$$\vec{V}_n \mid_\Gamma = 0, \quad (5)$$

wher Γ is the horizontal boundary. The subscript n represents exterior normal to the boundary Γ.

Under the lateral boundary condition (5), Eqs. (3) and (4) have some integral properties such as: (1) gross mass is conserved; (2) energy is conserved if the forcing and dissipation are omitted; (3) the nonlinear advection operators

are skew-symmetric; and (4) Coriolis force and curvature terms do not change the kinetic energy density.

In terms of those elementary discrete operators used by ZENG *et al.* (1987, 1990), we can get the difference equations on a C-grid which have the same integral properties as those of the continuum differential equations.

The model domain extends from 98.75° E to 69.75° W and from 60.25° N to 60.25° S as shown in Fig. 9b. We adopt idealized topography where the maximum water depth is taken to be 200 m, that is, we study a flat bottom barotropic ocean of 200 m depth which has realistic topography only for the shallow water regions such as the Bohai Sea, Yellow Sea and most of the East China Sea. Therefore, for the Pacific Ocean the model results mainly reveal the features of the upper layer circulation.

Most of the lateral boundaries are just the coastlines of Asia, North and South America. Those open boundaries to the north in the Bering Sea, to the southwest and to the south are replaced by closed boundaries. Along the northern and southern lateral boundaries we take $V=0$, while $U=0$ along the eastern and western boundaries.

The model horizontal grid size is chosen to be $\Delta\theta=0.5°$ and $\Delta\lambda=0.5°$, so that the total grid points are 384×242. The initial conditions are set as,

$$U=0,\ V=0,\ \phi=0 \text{ (i.e., } \zeta=0) \qquad (6)$$

The lateral eddy viscosity coefficient A_m is 10^7 cm^2/s and the bottom friction coefficient κ_2 is $3.3\times10^{-3}\times(u^2+v^2)^{1/2}/h$. Because our model is a free surface model, the timestep is greatly restrained by the surface gravity waves. In order to save computing time, we also adopt the splitting method used by ZENG *et al.* (1985) when integrating by taking $\Delta t_1=6$ min as a time step for the adjustment process and $\Delta t_2=60$ min for the processes of advection and dissipation.

Defining a generalized kinetic energy density $e_k=(U^2+V^2)/2$ and an available potential energy density $e_{ap}=\phi^2/2$, then the total kinetic energy is $KE=\int_s\int e_k ds$ and the total available potential energy is $PE=\int_s\int e_{ap} ds$, where s is the model domain and $ds\equiv a^2\sin\theta\, d\theta\, d\lambda$.

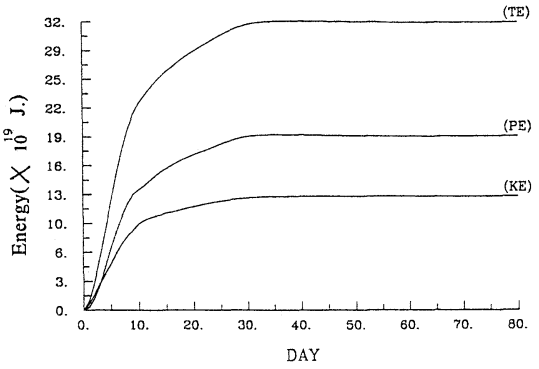

Fig. 1. Temporal variation of energy for January. PE: total available potential energy; KE: total kinetic energy; TE = PE + KE.

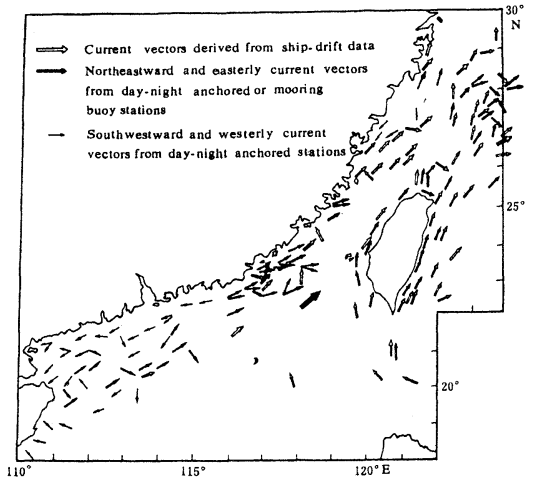

Fig. 2. Observed current vectors in winter off the southeast coast of China (from Guan, 1986).

Starting from the resting state represented by Eq. (6), the model forced by the monthly mean climatological wind stress (HELLERMAN and ROSENSTEIN, 1983) is integrated for 80 simulation days for each month. In order to examine the time dependent behavior of solutions, we also calculate the total kinetic energy and total available potential energy for each month. The temporal change of energy for January is shown in Fig. 1. Situations for other months are similar to Fig. 1. It can be shown from Fig. 1 that the total kinetic energy and the total available potential energy do not change appreciably after about 40 days. This indicates that the current speed and sea surface elevation at every point

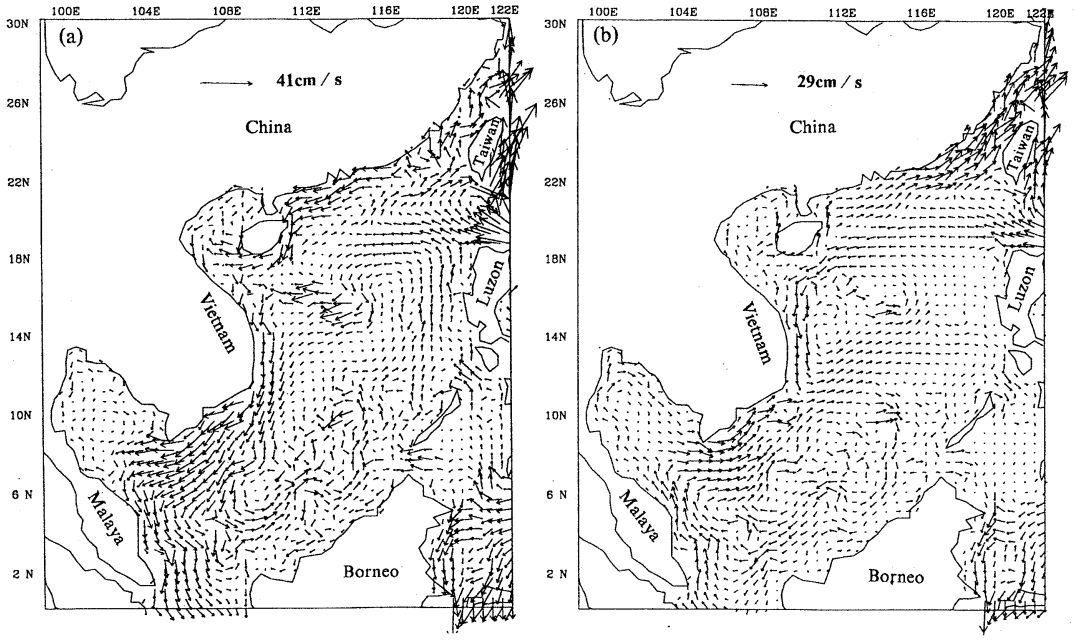

Fig. 3. Simulated depth mean velocity in South China Sea. (a) January, (b) July.

stay roughly the teady. Therefore, the results after 80 days of integration may represent the steady state upper layer circultation in the Pacific Ocean (i.e., the monthly mean current). From Fig. 1, we also observe that the total available potential energy corresponding to the sea surface elevations is greater than the total kinetic energy, which seems to indicate that the free surface model is more reasonable physically because it takes into account the transformation of the form of kinetic and available potential energy.

3. Results

Fig. 3 shows the computed monthly mean currents in the South China Sea (SCS). From Fig. 3a, it can be shown that under the intense influence of the northeasterly wind in winter, in the northern area of SCS, besides a leeward coastal current flowing southwestward, a windward current similar to the observed South China Sea Warm Current is very clearly visible. This current starts from the coastal region off the eastern Hainan Island flowing northeastward through Taiwan Strait and joining the Taiwan Warm Current. This strongly confirms the supposition raised by GUAN *et al.* (1964). In summer, a wide current also starts from the area off the eastern Hainan Island flowing northeastward through the Taiwan Strait and then entering the East China Sea as shown in Fig. 3b.

Fig. 5 shows the currents in the Bohai Sea, Yellow Sea and East China Seas as well as in the adjacent areas. It is evident from Fig. 5a that a branch of the Kuroshio north of Taiwan merges into the Taiwan Warm Current, and part of the water flow continuously along a cyclonic path and joins the left flank of the Kuroshio. Part of the Taiwan Warm Current flow northward reaching the southern edge of the Qiantangjiang Estuary, where it meets the extension of the Yellow Sea Coastal Current. They together turn to the east and flow northeastward. In the area northwest of Amami Oshima, the path of the Kuroshio exhibits an anticyclonic curvature, part of the Kuroshio water joining the northeast current mentioned above along the way to form a mixed water flowing east. In the area southwest of Kyushu, this current of the mixed water splits; the major branch turning to the southeast to merge the Kuroshio, and the other weaker branch being the Tsuhima Warm Current as described traditionally. The latter flows

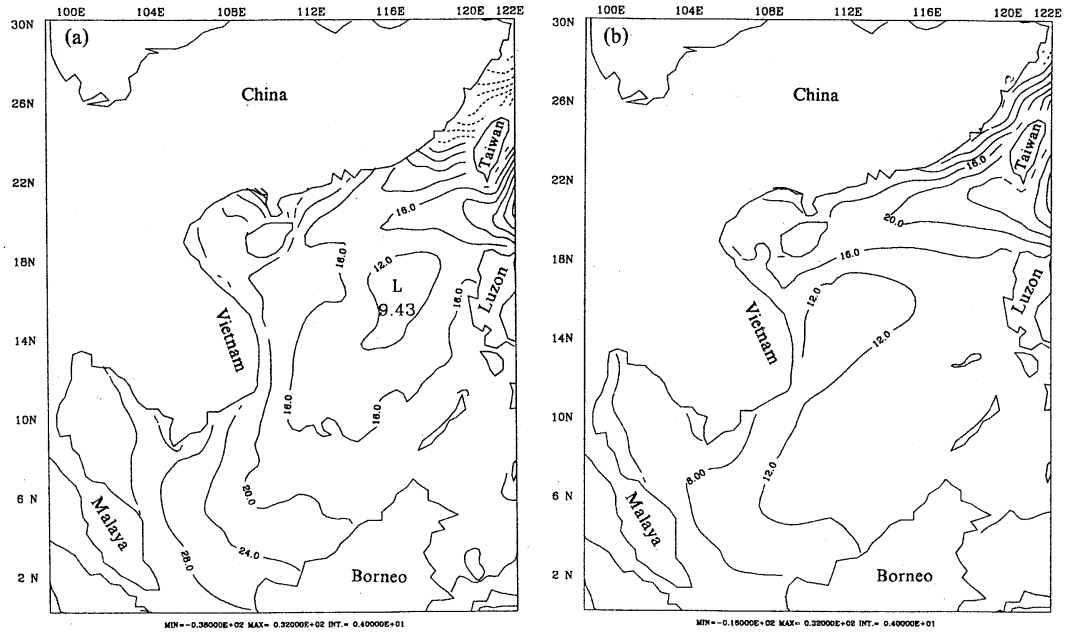

Fig. 4. Simulated sea surface elevation in the South China Sea. The contour interval is 4 cm. (a) January, (b) July.

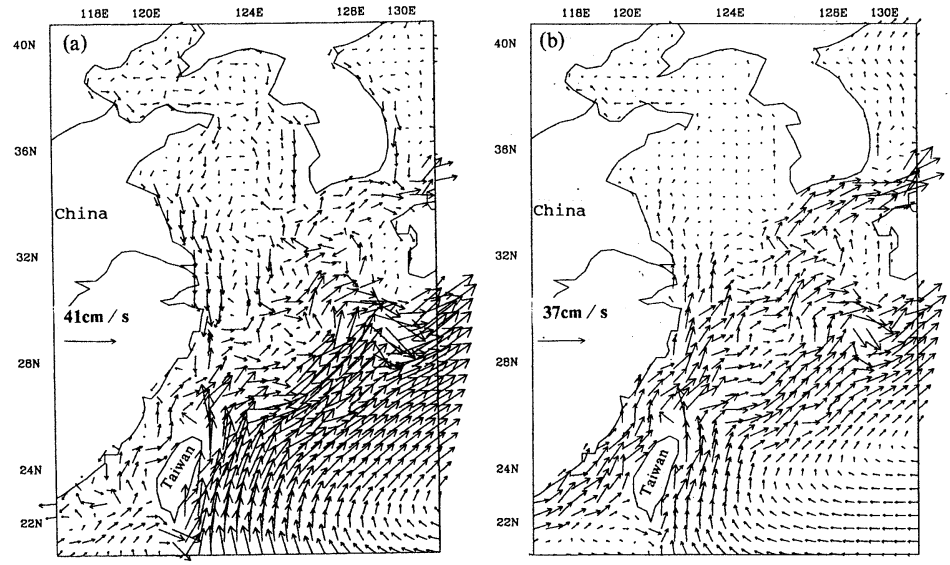

Fig. 5. Same as Fig. 3 but for the East China Sea and its adjacent area. (a) January, (b) July.

northward, passes through the Korea Strait and enters the Japan sea. Finally this current enters the Pacific Ocean through the Tsugaru Strait as shown in Fig. 7a.

It is obvious from Figs. 3a and 5a that the computed current patterns in the northern SCS and offshore region of eastern Zhejiang agree well with observations in Fig. 2.

In summer it can be clearly seen from Fig. 5b that from the Taiwan Strait to the Korea Strait the pattern of the northeastward flowing current is similar to that in winter except for a greater width. It moves into the Pacific Ocean mainly through the Soya Strait as shown in Fig.

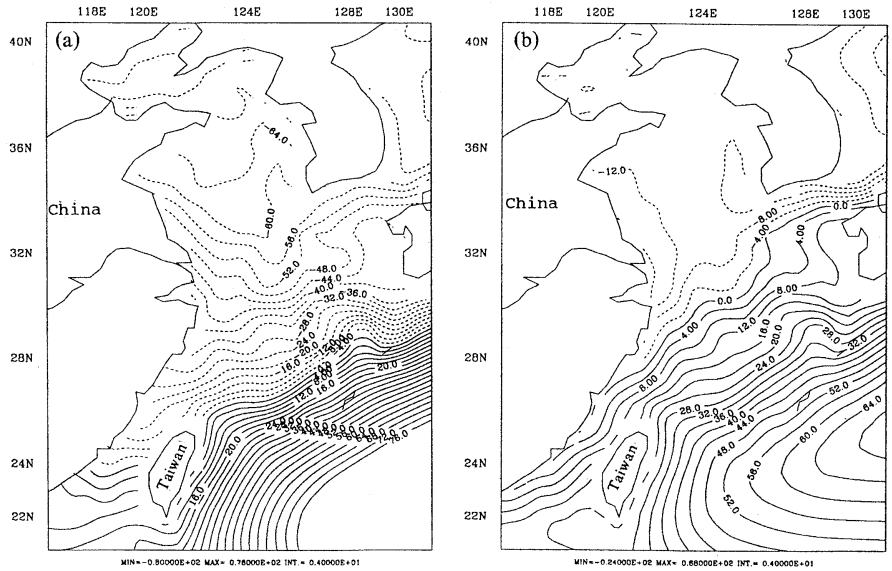

Fig. 6. Same as Fig. 4 but for the East China Sea and its adjacent area. (a) January, (b) July.

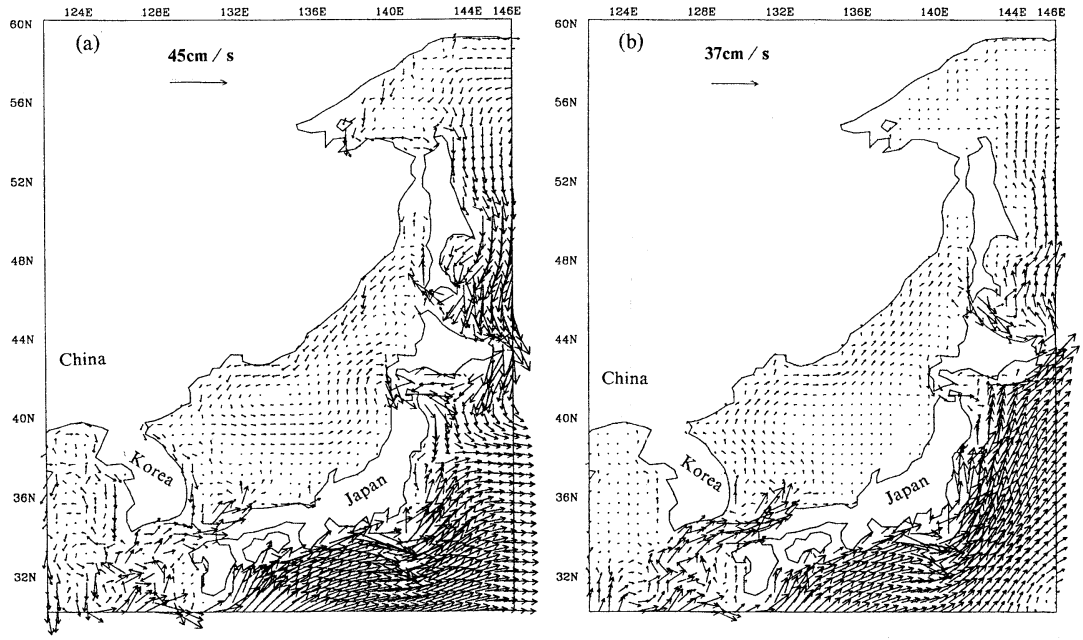

Fig. 7. Same as Fig. 3 but for the Japan Sea. (a) January, (b) July.

7b. We do not know whether it in reality passes, through the Soya Strait or not because we have no available observational data to confirm it. We were informed (TAKANO, private communication) that the Marine Environment Atlas–Currents in Adjacent Seas of Japan (compiled by Japan Oceanographic Data Center, published by Japan Hydrographic Association, 1973) shows that the flow is westward (from the Okhotsk Sea to the Japan Sea) in winter, and is eastward in spring, summer and fall, which is consistent with the model results in this paper.

From Fig. 5 we also see at about 30° N, 126° E that the winding current flows northward,

Table 1. Maximum and mean velocities as well as transports through the Taiwan and Korea Straits according to the model results.

month	Taiwan Strait			Korea Strait		
	$\|\vec{V}\|$ max(cm/s)	$\|\vec{V}\|$ mean(cm/s)	Q ($10^6 m^3/s$)	$\|\vec{V}\|$ max(cm/s)	$\|\vec{V}\|$ mean(cm/s)	Q ($10^6 m^3/s$)
Jan.	16.0	11.4	1.05	19.0	11.0	0.9
Jul.	23.0	15.8	2.07	32.0	19.3	2.2

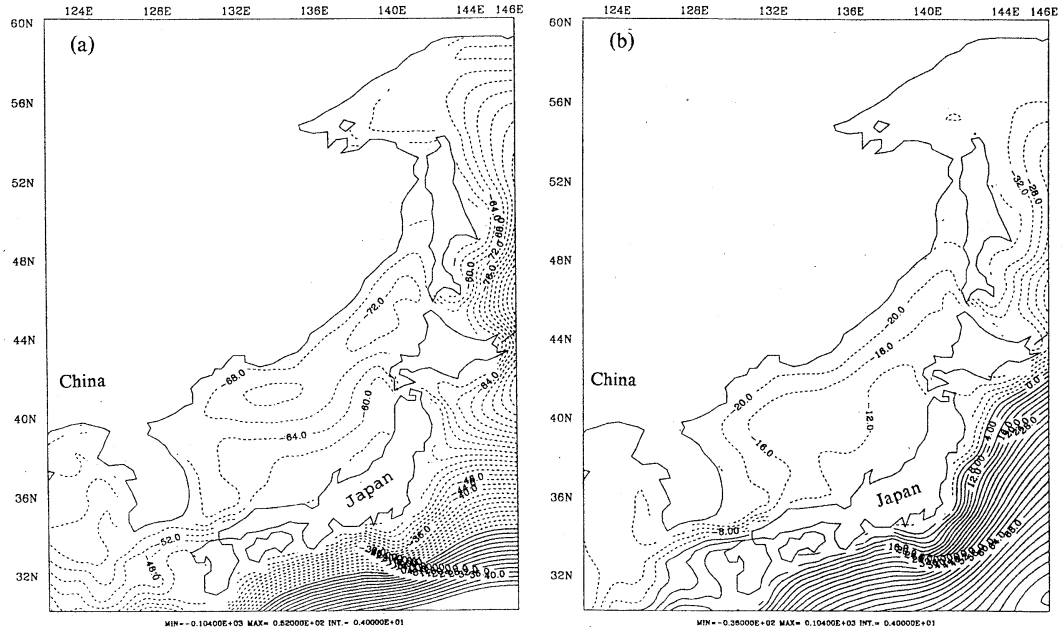

Fig. 8. Same as Fig. 4 but for the Japan Sea. (a) January, (b) July.

northeastward and then northwestward both in winter and summer. At about 32° 30′ N, 125° 30′ E, it turns to the northeast and fully enters the Korea Strait in summer, but it splits in winter into a small branch feeding the Yellow Sea to form the Yellow Sea Warm Current and another bigger one moving northeastward then entering the Korea Strait. In addition, there exists a cyclonic eddy in the northern East China Sea in winter. This windward current constitutes the western and northern flank of the cyclonic eddy.

On the basis of the above analysis it is evident that there indeed exists a long and narrow northeastward flowing current which starts from the region off the eastern Hainan Island, passing through the Taiwan Strait, East China Sea, the Korea Strait and Japan Sea finally entering the Pacific Ocean through the Tsugaru Strait in winter while through the Soya Strait in summer. Its proper name would be the "Hainan-Taiwan-Tsushima-Tsugaru/Soya Warm Current (HTTT/SWC)."

The maximum and mean values of the northeastward depth-averaged current velocity in the Taiwan Strait and Korea Strait as well as the volume transport through these two straits are given in Table 1. It is clear from Table 1 that the transport through the Taiwan Strait or Korea Strait is strong in summer but weak in winter, which is in good agreement with observations.

In order to facilitate the dynamical analysis, the computed sea surface elevations are given in Figs. 4, 6, 8 and 9. From these figures, it can be shown that the sea surface elevations are lower everywhere on the left of the "Hainan-Taiwan-Tsushima-Tsugaru/Soya Warm Current" but higher on the right of the current. Therefore, the sea surface slope is formed along the cross

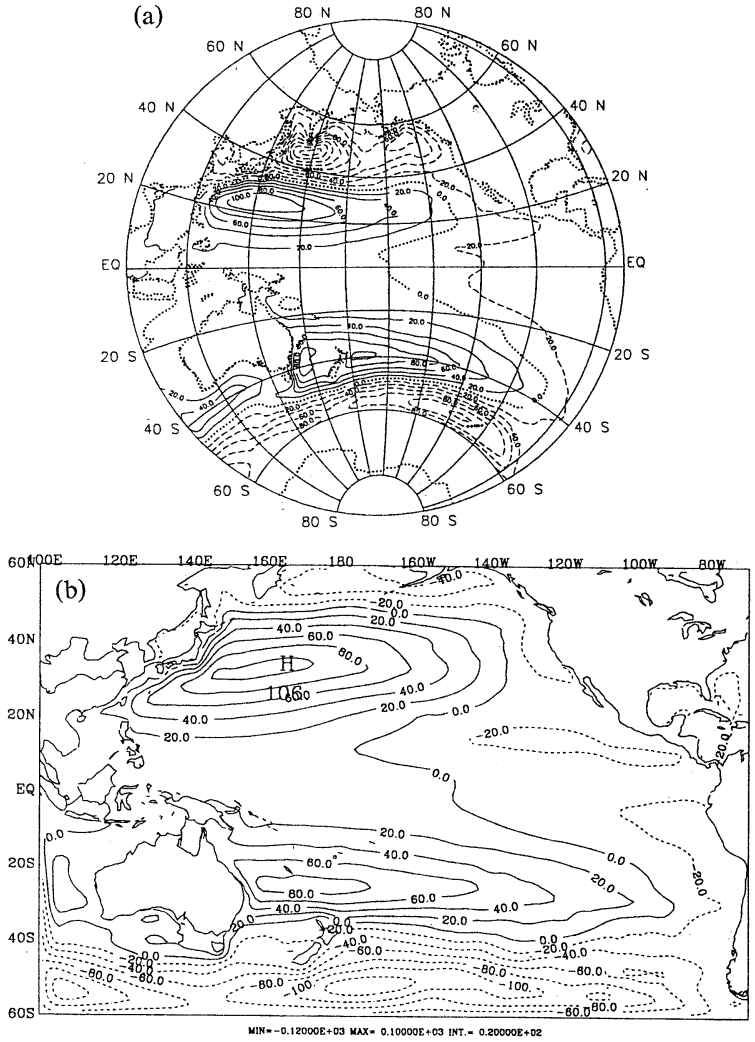

Fig. 9. Same as Fig. 4 but for the whole Pacific. (a) January, (b) July.

Table 2. Sea surface slope in the direction of the current, $\partial\zeta/\partial y$, and sea surface difference, $\Delta\zeta$, according to the computed results.

month	$\Delta\zeta$ (cm)			$\partial\zeta/\partial y$
	Hainan-Tsugaru	Hainan-Soya	Kitakyushu-Pusan	Shanwei-Tsushima
Jan.	90	84	13	-3.15×10^{-7}
Jul.	32	50	25	-1.4×10^{-7}

section of the current. The sea surface elevation differences, $\Delta\zeta$, between Kitakyushu and Pusan, between the area off the eastern Hainan Island and the area east of the Tsugaru/Soya Strait as well as the sea surface slope in the direction of the current, $\partial\zeta/\partial y$, from southeast of Shanwei to the central part of the Korea Strait along the axis of the current are given in Table 2.

Figs. 4, 6, 8 and 9 and Table 2, show that there exists not only the sea surface slope across the current, but also the sea surface slope in the direction of the current, the combined effect of

which may be one of the major forces driving the current. The friction at the bottom can counteract the pressure gradient force caused by the sea surface slope in the current direction, while the cross sectional slope from southeast to northwest can balance the Coriolis force and drives the northeastward current. From Fig. 9, it is obvious that these slopes of the sea surface are produced by the system of the wind-driven circulations in the Pacific Ocean.

4. Remarks

Based on the simulation results we make following remarks:

1. From the area off the eastern Hainan Island to the Tsugaru/Soya Strait, there exists a northeastward current both in winter and summer which may be driven by the sea surface slope both in the direction of the current and across the current from southeast to northwest.

2. The Tsushima Warm Current may be considered to originate mainly from the South China Sea Warm Current. In the area northwest of Amami Oshima, when flowing along an anticyclonic path, outer fringe water of the Kuroshio joins the northeastward current to form a mixed water flowing eastward. This current splits at about 30° N, 128° E and the major branch turns to the southeast and joins the Kuroshio again, while the minor branch flows northward which has been considered traditionally to be the origin of the Tsushima Warm Current. We believe that this weak northward branch is just a small part of the Tsushima Warm Current. It does not seem to be a direct branch of the Kuroshio. In fact, the water source of the Tsushima Warm Current mainly comes from the winding current which is further away from Kyushu.

3. The total available potential energy due to the fluctuation of the free sea surface is greater than the total kinetic energy (Fig. 1). Therefore, the effect of the pressure gradient caused by the fluctuation of the sea surface on the upper layer currents is also very important, which could not be examined rigorously not only because of the lack of observational data of the sea surface elevation, but also because of the omission of the sea surface fluctuation by the bottom topography.

4. Due to ignoring the effects of temperature, salinity and the variation of density in the model, simulated currents are mainly governed by such factors as wind stress, topography of the continental shelf, β-effect, nonlinear effect and coastal configuration. In order to reveal completely the formation mechanism of the currents, simulations should be carried out for a baroclinic ocean model based on the full primitive equations in the future.

Acknowledgments

The authors wish to thank Prof. B.X. GUAN and X.H. ZHANG for helpful discussions and valuable comments, Dr. Z.J. ZANG, N. BAO and Z.X. LONG for providing the plotting routines, Miss X. WANG and Y.B. SUN for typing the manuscript.

References

FANG, G. and B. ZHAO (1988): A note on the main forcing of the northeastward flowing current off the southeast China coast. Prog. Oceanogr., **21**, 363–372.

FANG, G., B. ZHAO and Y. ZHU (1989): Water transports through the Taiwan Strait and East China Sea measured with current meters. *In* Programme and Abstracts. Fifth JECSS, Workshop, Kangnung, Korea, p30.

GUAN, B.X. (1984): An evidence for the current flowing northward against wind in winter in the East China Sea and South China Sea. Report of the study and investigation for the Bohai, Yellow and East China Seas, 142–150 (in Chinese).

GUAN, B.X. (1986a): A sketch of the current structures and eddy characteristics in the East China Sea. Studia Marina Sinica, **27**, 1–21 (in Chinese with English abstract).

GUAN, B.X. (1986b): Evidence for a counter-wind current in winter off the southeast coast of China. Chin. J. Oceanol. Limnol., **4**, 319–332.

GUAN, B.X. and S.J. CHEN (1964): The current systems in the near-sea area of China Seas. Report of the Chinese National Comprehensive Oceanographic Survey, 1–85 (in Chinese).

GUAN, B.X., D. WENLAN and H. MAO (1964): The winter surface current systems of the southern Huanghai Sea and the northern East China Sea and discussions of some related problems. (In Chinese)

HELLERMAN, S. and M. ROSENSTEIN (1983): Normal monthly windstress over the world ocean with error estimates. J. Phys. Oceanogr., **13**, 1093–

1104.

ZENG, Q.C. (1983): Some numerical ocean-atmosphere coupling models. Proceedings of the First International Symposium on Integrated Global Ocean Modelling, Tullin, USSR.

ZENG, Q. C. and X. H. ZHANG (1987): Available energy conservative finite-difference schemes for baroclinic primitive equations on sphere. Chinese Journal of Atmospheric Sciences, **11**, 121–142.

ZENG, Q.C., Z.Z. JI and R.F. LI (1985): A numerical model of offshore currents and some tests. Proceedings of the International Symposium on Oil Development Enviroment of the South China Sea, 15–21.

ZENG, Q.C., X.H.ZHANG, C.G.YUAN, R.H.ZHANG, N. BAO and X.Z. LIANG (1990): IAP ocean general circulation models. Proceedings of the Third International Summer Colloquium on Climate Change Dynamics and Modelling, 331–350.